0254-6124/2022/42(6)-1171-14 *Chin. J. Space Sci.* 空间科学学报

YANG Zhe, SHEN Guohong, JING Tao. Development of High-energy Particle Detectors for Space Exploration. *Chinese Journal of Space Science*, 2022, **42**(6): 1171–1184. DOI:10.11728/cjss2022.05.210611068

Development of High-energy Particle Detectors for Space Exploration

YANG Zhe[1,2,3,4] SHEN Guohong[1,3,4] JING Tao[1,3,4]

1(*National Space Science Center*, *Chinese Academy of Sciences*, *Beijing* 100190)

2(*University of Chinese Academy of Sciences*, *Beijing* 100049)

3(*Beijing Key Laboratory of Space Environment Exploration*, *Beijing* 100190)

4(*Key Laboratory of Science and Technology on Space Environment Situational Awareness*, *Chinese Academy of Sciences*, *Beijing* 100190)

Abstract Space environment exploration is a hot topic globally. The scope of space exploration ranges from near-Earth space to the moon, other planets in the solar system, and even the heliosphere and interplanetary space. It is used for various crucial applications, including aerospace technology development, space weather research, understanding the origin and evolution of the universe, searching for extraterrestrial life, and finding human livable places. Although China's space environment exploration started late, its progress has been rapid. China is gradually narrowing the gap with advanced countries and may eventually lead the world in space research. This article briefly reviews the development history of China's space environmental detectors.

Key words High-energy particle detectors, Near-Earth space exploration, Lunar exploration, Space environment

Classified index V476.1

0 Introduction

The high-energy space radiation, including galactic cosmic rays, solar high-energy particles, and Earth's radiation belt particles, is one of the vital factors that directly affect the normal operation of spacecraft and threaten the safety of astronauts. The electronic systems of spacecraft are damaged by high-energy particles, which include radiation damage effects and single event effects[1]. Such damage can lead to the degradation or failure of spacecraft performance and even lead to catastrophic consequences. In addition, long-term excessive radiation accumulation can cause irreversible damage to human organs and tissues. Therefore, the study of the high-energy radiation environment in space is an indispensable part of space exploration, which can provide a reliable design for the safety of spacecraft and astronauts. Furthermore, the detection of space radiation provides useful experimental data for understanding the structural characteristics of the physical field and the interaction between particles and field. Chinese space environment exploration has gone through decades of development. In this study, we have reviewed the progress history of China's space exploration.

1 Near-Earth Space Environment Exploration

1.1 China Manned Space Project

China Manned Space Project (CMSP) has paid great at-

Received June 7, 2021. Revised March 22, 2022

E-mail: shgh@nssc.ac.cn

tention to protecting the space environment since its early launch stage. The Space Environmental Monitors (SEMs) have been manufactured since the development of Shenzhou-II aircraft. SEMs aim to monitor the space weather in the orbit of the space station. SEMs can provide an early warning of catastrophic radiation events, thereby ensuring the safety of astronauts and normal operation of the spacecraft.

1.1.1 Shenzhou Manned Spacecraft

The SEM on Shenzhou-II and Shenzhou-III spacecraft includes an atmospheric density detector, an atmospheric composition detector, and a solid track detector to detect changes in the orbital atmosphere and the heavy-ion radiation. Apart from these detectors, the Shenzhou-IV and Shenzhou-V spacecraft are also equipped with a High Energy Proton And Heavy Ion Detector (HEPHID), a High Energy Electron Detector (HEED), a single event detector, a Low Energy Particle Detector (LEPD), and two surface potential detectors. The SEMs monitor the radiation environment of high-energy particles in the spacecraft orbit and provide warning for catastrophic radiation events, which ensures normal operation of the instrument and safety of astronauts[2]. The SEMs focus on the systematic detection of charged particles and their effects in the upper atmosphere to further understand the space weather conditions. The High-energy Particle Detectors (HPD) of the SEMs in the first phase of manned spacecraft provide the energy spectrum and spatial distribution of high-energy particles in the orbital space. Among them, HEPHID is used to monitor the high-energy protons, alpha particles, and other heavy particles in the orbit of the aircraft. The energy spectrum and spatial distribution of ions can detect protons in the energy range of 2.9～300 MeV, alpha particles in the range of 4～26 MeV per nucleon, and other heavy ions. The HEED is used to monitor the spatial distribution and energy spectrum of high-energy electrons in the orbital space in the energy range of 0.2～5 MeV[3]. The energy range of Shenzhou-IV/V HEED and HEPHID is shown in Table 1[4].

Shenzhou-IV/V HEPHID and HEED have provided several interesting results. During the quiet period of the space environment, high-energy particles in the manned space orbits are mainly distributed in the anomalous zone of the South Atlantic Ocean. There are only a few protons with energy greater than 3 MeV per second, and the count rate of electrons with an energy of 0.4～0.5 MeV count is 400 s^{-1}. As the energy increases, the flux of high-energy electrons and high-energy protons decreases rapidly. During solar proton events and geomagnetic storms, a large number of charged particles settle over high magnetic latitudes such as North America and southwestern Australia. After the solar proton event and magnetic storm, the intensity and flux of the charged particles in the radiation belt are extremely high, and such events can last for several days[5]. High-energy charged particles also have obvious directionality, especially high-energy electrons. A large number of particles are distributed perpendicular to the magnetic field lines[6].

Table 1 Energy range channels of Shenzhou-IV/V HEED and HEPHID

HEED	HEPHEI
E1: 0.20～0.40 MeV	P1: 2.9～4.0 MeV
E2: 0.50～0.60 MeV	P2: 4.0～5.4 MeV
E3: 0.60～0.80 MeV	P3: 5.4～8.0 MeV
E4: 0.80～1.00 MeV	P4: 8.0～15 MeV
E5: 1.00～1.30 MeV	P5: 15～26 MeV
E6: 1.30～1.60 MeV	P6: 26～32 MeV
E7: 1.60～2.00 MeV	P7: 32～60 MeV
E8: 2.00～5.00 MeV	P8: 60～100 MeV
	P9: 100～160 MeV
	P10: 160～300 MeV
	Heavy ions: 4～26 MeV per nucleon
	α particles: 4～26 MeV per nucleon

1.1.2 Space Laboratory Missions

The second phase of the manned spacecraft Tiangong-I and Tiangong-II is also equipped with a Particle Direction Detector (PDD), which is composed of a proton energy spectrum sensor, an electron energy spectrum sensor, and 16 directional flux sensors. A picture of PDD is shown in Fig.1.

Some parameters of these sensors are listed in Table 2[7]. The PDD monitors the energy spectrum distribution, direction distribution, regional distribution, and temporal and spatial changes of high-energy particles in the orbit of the spacecraft[7]. Thus, complete radiation images of high-energy charged particles in the or-

bital space can be obtained. These results provide more accurate data for the establishment of static and preliminary dynamic particle radiation models of manned spacecraft.

Tiangong-I is the first prototype space station in the world that can measure high-energy electron and proton intensities in 16 directions in the manned space orbit. At the same time, it also provides sufficient reference data for China's subsequent manned space missions to enter this orbit. Fig.2 and Fig.3 show the direction distribution of high-energy electrons and protons measured by the Tiangong-I PDD, respectively. The results of Tiangong-I and Tiangong-II are generally consistent during the quiet period of solar activity.

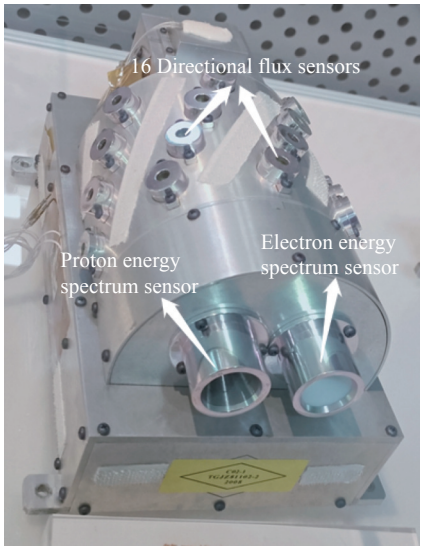


Fig. 1 Picture of the space particle direction detector

Table 2 Main parameters of the PDD

	Directional flux sensor	Electron energy spectrum sensor	Proton energy spectrum sensor
Energy range	High-energy electrons: > 100 keV High-energy protons: 1.5～200 MeV	0.2～10 MeV	3～300 MeV
Field of view	180°×15°	30°	40°

1.1.3 China Space Station

The construction of the space station is the third step of the "three-step strategy" development of the CMSP[8]. The China Space Station (CSS) project is being implemented in two phases: the space laboratory mission and the space station mission. Presently, China has completed the space laboratory phase mission and entered the space station mission phase. The CSS is a manned space station, consisting of a core module and two experimental modules. It will operate in low-Earth orbit for a long time. The orbit is a near-circular orbit with an inclination of 42°～43° and an altitude of 340～450 km. The core module of the CSS was successfully launched in Wenchang, Hainan on 29 April 2021.

To ensure the safety of astronauts and the space station, an SEM is installed in the experimental cabin. The SEM is used for comprehensive monitoring of particle radiation, orbital atmosphere, and plasma charging and discharging. According to the characteristics of the different stages of the space station and various application requirements, the Energy Particle Detector (EPD) in the experimental cabin I will be used to detect particle radiation. A schematic of the EPD structure is shown in Fig.4. The measured particle species include protons, electrons,

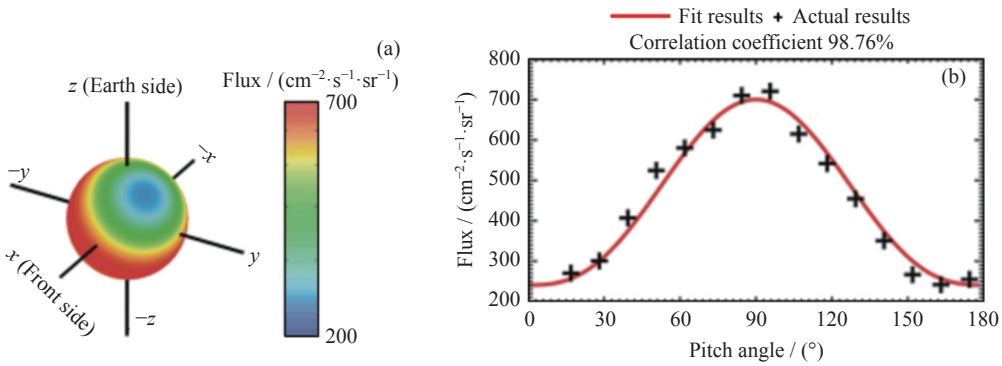


Fig. 2 Direction distribution of high-energy electrons measured by Tiangong-I PDD. (a) Electron radiation intensity of Tiangong-I in the center of the South Atlantic anomaly zone in different directions. (b) Distribution of electron fluxes (>35 keV) in the center of the South Atlantic anomaly zone with the pitch angle

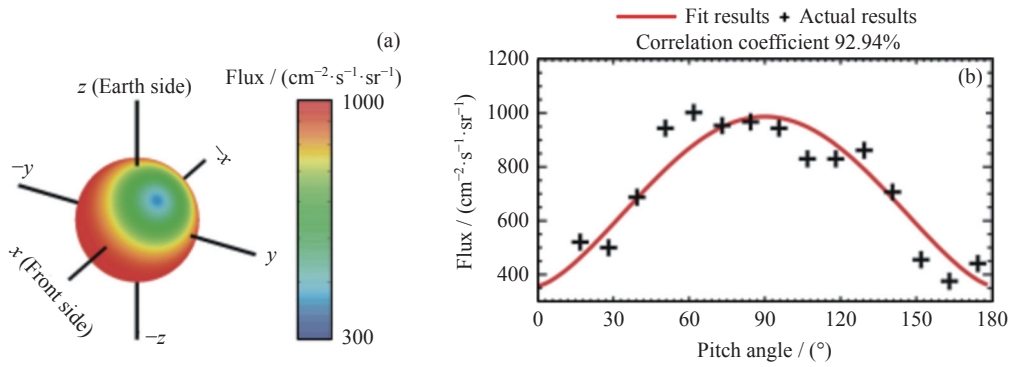


Fig. 3 Direction distribution of high-energy proton measured by Tiangong-I PDD. (a) The proton radiation intensity of Tiangong-I in the center of the South Atlantic anomaly zone in different directions. (b) The distribution of proton fluxes (1.5～200 keV) in the center of the South Atlantic anomaly zone with the pitch angle

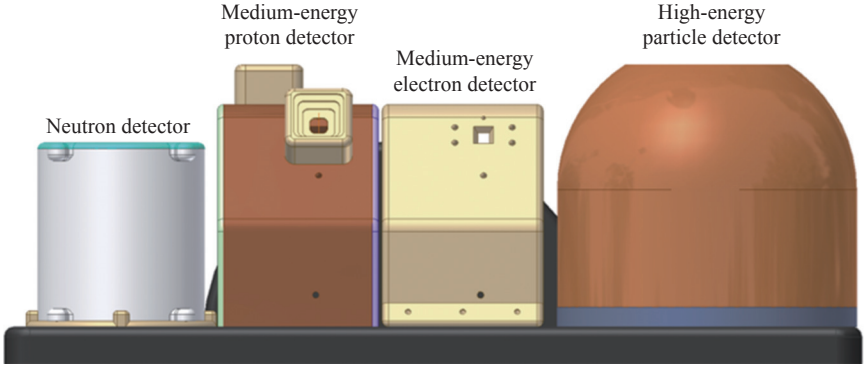


Fig. 4 Schematic structure of energy particle detector

heavy ions, and neutrons, and the energy range is from medium to high energy. The measured physical quantities include energy spectrum, flux, directional characteristics, Linear Energy Transfer (LET) spectrum and dose rate, *etc*. Some technical indicators of the EPD are shown in Table 3. Through comprehensive monitoring of the space environment, EPD provides necessary input data for examining the long-term changes and disturbance characteristics of the space environment of the manned space orbit. In addition, it is also conducive to further improving the manned space engineering and adaptability of the space environment.

1.2 Fengyun Series of Meteorological Satellites

As early as the 1970s, China began to implement a meteorological satellite program. By the end of 2020, it launched 18 meteorological satellites (including 9 polar-orbiting satellites and 9 geostationary satellites). Recently, the FY-4B satellite was successfully launched on 3 June 2021. The commercial operation of polar-orbiting satellites and geostationary satellites has been realized. FY-2 and FY-3 have become important members of the global operational meteorological satellite detection system. They are important tools of China for global data monitoring, regional weather and environmental monitoring, meteorological services, and scientific research on the Earth system. Some meteorological satellites of the Fengyun series are equipped with SEM, which can monitor the flux of solar X-rays, high-energy protons, high-energy electrons, and high-energy heavy ions. The SEMs are used for space weather monitoring, early warning, and forecasting operations. The SEMs on the FY-1 and FY-3 series include HPDs and ionospheric measurement sensors. The FY-2 and FY-4 series satellites are also equipped with SEMs to monitor solar activity and environment of high-energy charged particles in the geostationary orbit and provide early warning and forecast of solar flares, solar proton events, and high-energy electron storms[9].

1.2.1 Polar-orbiting Meteorological Satellites

The FY-1 and FY-3 series satellites are meteorological

Table 3 Some parameter indices of Experimental Module I

Parameter type		Parameter index
Energy spectrum range	Protons	20 keV～300 MeV
	Heavy ions	8～400 MeV per nucleon
	Electrons	20 keV～10 MeV
	Neutrons	0.025 eV～100 MeV
Particle composition discrimination		Distinguish protons, heavy ions He～Fe ($2 \leqslant Z \leqslant 26$), electrons, and neutrons
LET spectrum range		0.001～75 MeV·mg·cm^{-2} (≥64 channels)
		>75 MeV·mg·cm^{-2} (1 channel)
		Precision: better than 15%
Dose rate		0.01～100 rad·d^{-1}(Si)

satellites operating in sun-synchronous polar orbits. The FY-1 meteorological satellite is the first transmission-type polar-orbiting remote sensing satellite in China. It is the first step to develop and launch a space-based remote sensing application satellite. The space particle component detector onboard is used to monitor high-energy particles in sun-synchronous orbit space. The high-energy proton and heavy-ion radiation data are useful for flight control management, anomaly analysis, and the satellite's anti-radiation reinforcement design. The SEM monitors one channel of high-energy electron fluence, five channels of high-energy proton flux (energy spectrum), and six channels of heavy-ion components. The monitored heavy-ion components range from helium ions to iron ions (atomic numbers 2～26) and are divided into six levels according to the atomic number, and the lightest ions in each level are He, Be, C, Mg, Ar, and Fe[10].

The FY-3 satellites are second-generation polar-orbiting meteorological satellites. They are developed and improved based on the FY-1 technology. The ability to accurately detect global, all-weather, multi-spectral, and three-dimensional characteristics of the surface state has improved the quality of weather forecasts in China, other Asian countries, and the world. The level of natural disaster and environmental monitoring has been improved significantly. The SEM onboard FY-3 is improved based on the FY-1 SEMs, which has enhanced the detection accuracy of high-energy particles and broadened the particle measurement range. The SEMs can effectively monitor the space environment and the flux of high-energy charged particles in real-time, and it records the impact of space weather on the satellites. Table 4[10–12] shows some parameters of SEMs of the Fengyun polar-orbiting satellites.

Fig.5 shows the global distribution of FY-3C high-energy protons from 1 to 16 in October 2013. It can be seen that during periods of relatively calm space weather, high-energy protons are mainly distributed in the anomalous area of the South Atlantic Ocean. Near the center of the South Atlantic anomaly, the proton flux is higher. As the proton energy increases, its distribution range and flux decrease. The South Atlantic anomaly is formed due to the abnormal structure of the geomagnetic field, and the high-energy particles captured by it are part of the inner radiation belt. The South Atlantic anomaly has a significant impact on the low-orbiting spacecraft.

Fig.6[12] shows the global distribution of FY-3C high-energy electrons from 16 October to 15 November 2013. It can be seen that high-energy electrons are mainly distributed in the anomalous and polar regions of the South Atlantic. With the increase in the electron energy, its distribution range and flux also decrease gradually. Especially, in the polar region, the decrease is rapid. The trapping mechanism of electrons in the South Atlantic anomaly is similar to that of protons. The high-energy electrons in the polar region are mainly sinking electrons in the outer radiation zone, and their distribution is affected by solar and geomagnetic activities.

Li *et al.*[12] compared the FY-3C high-energy particle data with NOAA-18 and FY-3B satellite data during the calm period of space weather. The results verified the stability of the SEM state and also confirmed that the high-energy particle data of the FY-3C satellite has good consistency with the data of other satellites.

1.2.2 Geostationary Meteorological Satellites

China began to develop geostationary orbit meteorological satellites and ground application systems in the 1980s. The first geostationary meteorological satellite FY-2A was launched on 10 June 1997 using the Long March 3 carrier rocket in Xichang. The FY-2 series satellites are the first generation of geostationary meteorological satellites in China, which work in the geosta-

Table 4 Some parameters of SEMs of Fengyun polar-orbiting satellites

	Electrons	Protons	Heavy-ions
FY-1C/D	E >1.6 MeV	P1: 2.9～102 MeV	He: 12～102 MeV
		P2: 5.4～11.7 MeV	Be: 30～320 MeV
		P3: 11.7～40 MeV	C: 60～570 MeV
		P4: 40～100 MeV	Mg: 0.2～1.7 GeV
		P5: 100～300 MeV	Ar: 0.3～2.8 GeV
			Fe: 0.5～2.3 GeV
FY-3A(B)	E1: 0.15～0.35 MeV	P1: 3.0～5.0 MeV	He: 11.6～104 MeV
	E2: 0.35～0.65 MeV	P2: 5.0～10 MeV	Li: 24.5～215 MeV
	E3: 0.65～1.2 MeV	P3: 10～26 MeV	C: 61～590 MeV
	E4: 1.2～1.9 MeV	P4: 26～40 MeV	Mg: 0.195～1.2 GeV
	E5: 1.9～5.6 MeV	P5: 40～103 MeV	Ar: 0.29～2 GeV
		P6: 103～308 MeV	Fe: 0.49～2.0 GeV
FY-3C(D)	E1: 0.15～0.35 MeV	P1: 3.0～5.0 MeV	He: 12～110 MeV
	E2: 0.35～0.65 MeV	P2: 5.0～10 MeV	Li: 24～220 MeV
	E3: 0.65～1.2 MeV	P3: 10～26 MeV	C: 61～570 MeV
	E4: 1.2～2.0 MeV	P4: 26～40 MeV	Mg: 0.2～1.2 GeV
	E5: 2.0～5.7 MeV	P5: 40～100 MeV	Ar: 0.3～2 GeV
		P6: 100～300 MeV	Fe: 0.5～2.0 GeV

tionary orbit in a spin-stabilized manner. The geostationary orbit is located at the edge of the center of the extraterrestrial radiation belt[13]. There are abundant high-energy charged particles, which threaten the safe operation of satellite instruments.

The SEM onboard FY-2 satellites can monitor and provide a warning on the changes in solar activity and disturbance of particles in the geostationary orbit in real-time. The SEM can provide early warning of disastrous space weather events, ensuring the safe operation of space-borne instruments. The SEM consists of a HPD and a solar X-ray detector. It can realize real-time monitoring of the multi-energy range of high-energy electrons, high-energy protons, high-energy heavy ions, and solar X-ray fluxes. The HPDs of the FY-2 01 batch of satellites (including FY-2A and FY-2B) are used to monitor the flux disturbance and energy spectrum distribution of high-energy protons, electrons, and heavy ions in the space environment of the satellite orbit. There are seven energy channels in total, including one electron energy channel, four proton energy channels, and two heavy ion energy channels. The high-energy particle monitors of the FY-2 02 batch satellites (including FY-2C, FY-2D, and FY-2E) have increased the detection efficiency of high-energy electron energy channels based on the FY-2 01 batch, including two high-energy electron energy channels, three high-energy electron energy channels, one proton energy channel, one heavy ion energy channel, and one alpha particle energy channel. FY-2 03 batch satellites (including FY-2F, FY-2G, and FY-2H) are equipped with a HEED and a HEPHID for high-energy electron and proton detection, which broadened the energy spectrum and refined the energy channels[14]. Pictures of HEED and HEPHID of FY-2F(G) are shown in Fig.7.

The FY-4A satellite is the first satellite of China's second-generation geostationary meteorological satellite, which uses three-axis stable attitude control. Compared with the stable-spinning FY-2 meteorological satellite, the performance of the FY-4A satellite is significantly improved. The SEM onboard the satellite monitors solar activity and space environment. The detection results provide data support for space weather forecast operation and research. The design of the HPD carried by the FY-4 satellite is completely different from that carried by the FY-2 series satellites. The FY-4 HPD is composed of six telescopes and electronic systems. Three telescopes are used for the detection of low-energy elec-

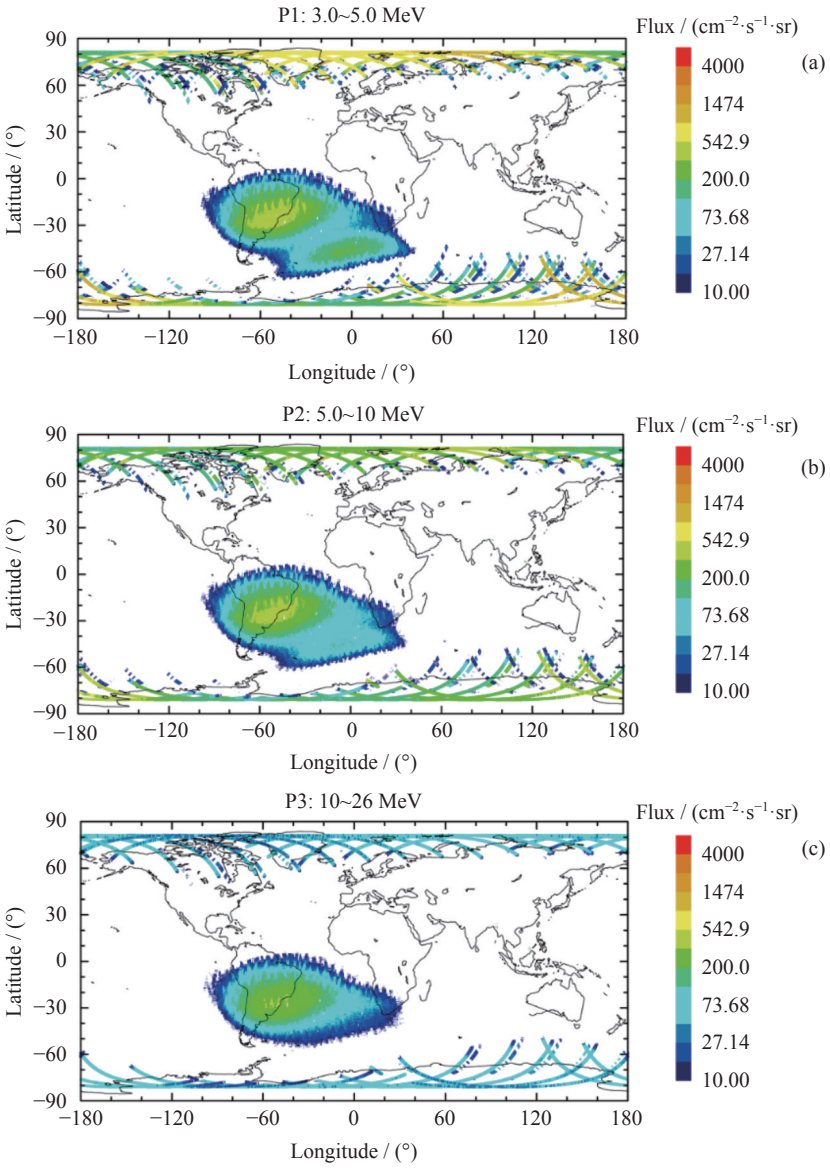


Fig. 5 Global distributions of FY-3C protons from 1 to 16 October 2013

trons (0.4～1.5 MeV), and one telescope is used for the detection of high-energy (>1.5 MeV) electrons. For detection, two telescopes are used to detect the energy spectrum of high-energy protons (1～4 MeV and 4～165 MeV). Fig.8 shows a picture of HPD onboard FY-4A. Table 5 shows the detected particle species and energy range of the SEMs of Fengyun Stationary Meteorological Satellite.

Liu *et al.*[15] compared and fused the observation data of relativistic electrons obtained by FY-4A and GOES-13 in the same orbit to eliminate the deviation between the two detection systems. Fig.9[15] shows the changes in the electron fluence of two satellites with energy greater than 2 MeV in the same period as a function of time. It can be seen that the observation results of the two satellites exhibit obvious diurnal changes. Since the time difference between the locations of the two satellites is 12 h, the phase changes of the electron fluxes observed by the two satellites in the figure are opposite, *i.e.*, the trends of the electron fluxes observed by the two satellites are the same.

1.3 Double Star Program

The Double Star Program (DSP) is a joint geospace exploration program between the China National Space Administration (CNSA) and the European Space Agency (ESA). The DSP uses the Cluster II four satellites of

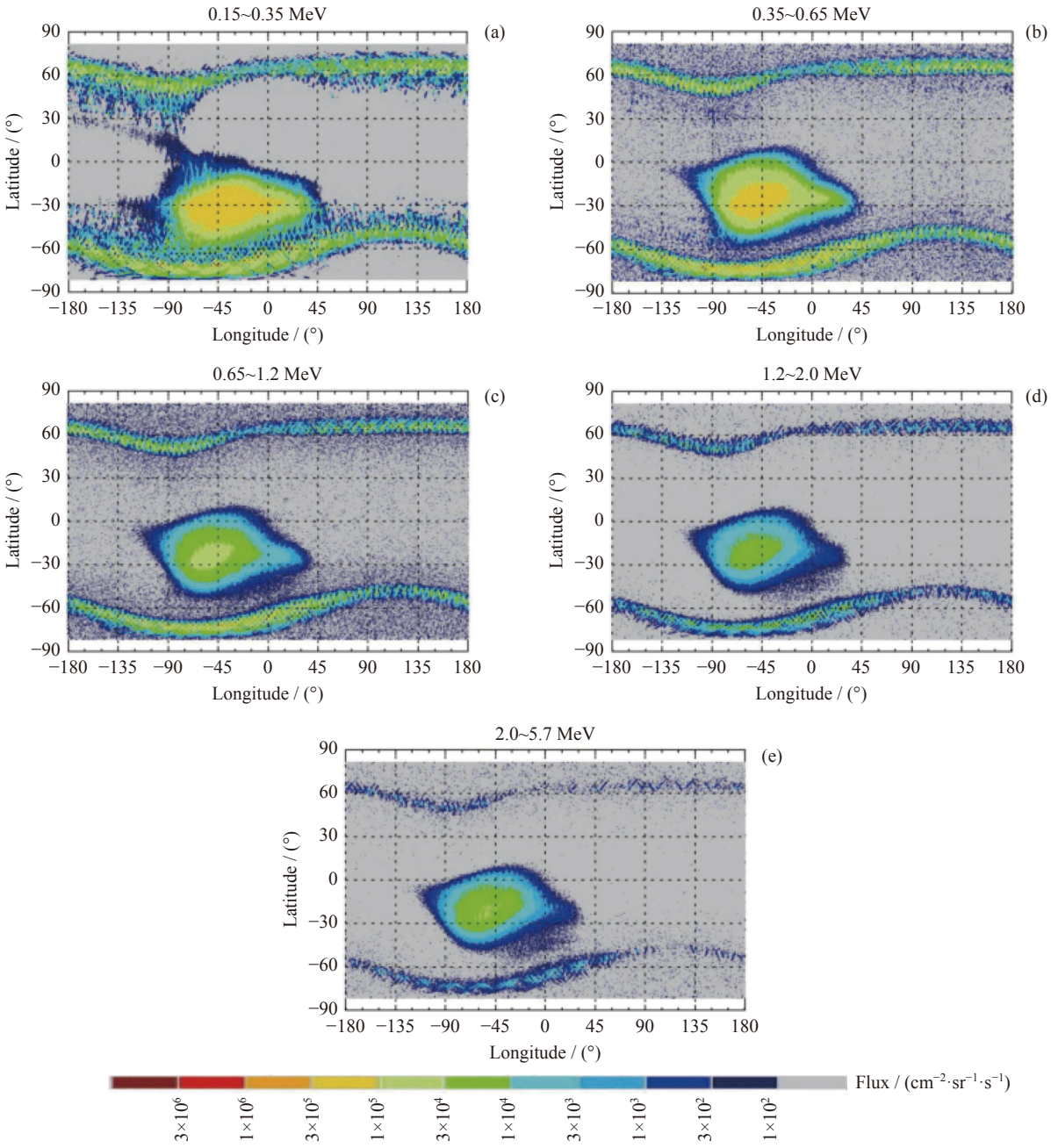


Fig. 6 Global distributions of FY-3C electrons from 16 October to 15 November 2013

ESA to complete the "six-point observation" of the Earth in space. The DSP includes two satellites: TC-1 operating in the near-Equator active area and TC-2 in the near-Earth polar active area[16]. Each satellite is equipped with three HPDs: a HEED, a High-Energy Proton Detector (HEPD), and a HID[17]. The main parameters of HEPDs onboard TC-1/2 are shown in Table 6[18]. Fig.10 shows a picture of the flight model of HEPD onboard TC-1. The detection results are used to analyze the distribution function, flux spectrum, and composition of high-energy particles for studying the temporal variation as well as temporal and spatial distribution characteristics of various particles during magnetospheric space storms[19].

Cao *et al.*[18] introduced some preliminary detection results and compared the directional flux of HEPD/TC-1 and AP8-predicted high energy proton omni-directional flux. Fig.11[18] shows the comparison result. It can be seen that the peak position and overall variation trend of the data obtained by HEPD are consis-

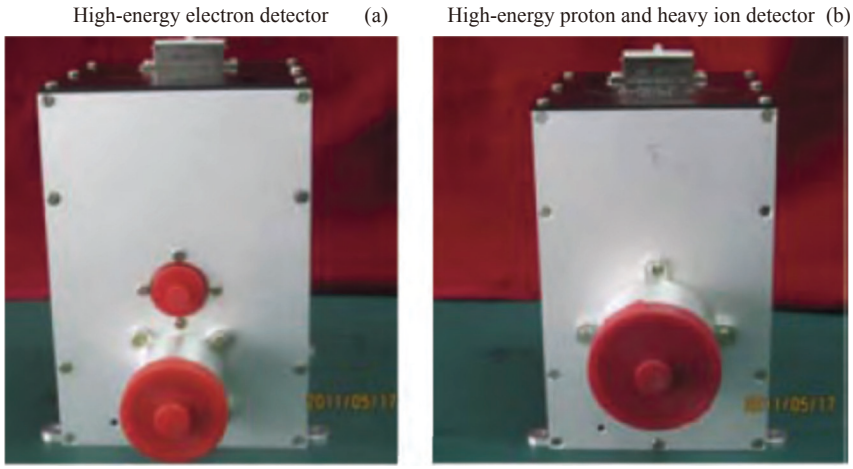


Fig. 7 High-energy electron detector, high-energy proton and heavy ion detector of FY-2F(G)



Fig. 8 High-energy particle detector of FY-4A

tent with the predicted result of the AP8 model, thereby verifying the reliability of the HEPD detection data.

2 Chinese Lunar Exploration Program

Chang'E-1 (CE-1) is the Chinese first lunar exploration satellite. The SEM onboard CE-1 is composed of a solar HPD and two Solar Wind Ion Detectors (SWIDs)[20]. They are used to detect composition, flux, energy spectrum, and time-varying characteristics of high-energy charged particles during the flight from the earth to the moon and around the moon[21]. HPD and SWIDs work together to accomplish the scientific goal of exploring the Earth-Moon space environment. The Chang'E-2 (CE-2) satellite is the pilot star of the second phase of the Chinese Lunar Exploration Program (CLEP). It flew out of the lunar orbit after completing various scheduled exploration tasks. CE-2 conducted some extended experiments such as the Sun-Earth Lagrangian L2 point exploration and the Tuatatis asteroid flyby, becoming an artificial asteroid orbiting the sun. The SEM onboard CE-2 satellite has the same parameters as that onboard the CE-1 satellite. The orbiting period of CE-2 was the peak year of solar activity, which provided the best exploration opportunity for detecting and studying solar wind, coronal mass ejection, solar energetic particles, and their impact on the lunar space environment. Fig.12 shows the SEM onboard CE-1.

SWID adopts a hemispherical electrostatic analyzer with 12 detection entrances evenly distributed on a fan with a polar angle of 180°. Each polar angle entrance divides the energy channel width of 0.04～20 keV into 48 energy channels in a nearly logarithmic manner. The field of view is 180°×6.7°, the angular resolution is 15°×6.7°, the time resolution can reach 2.9 sec, and the counting range is 0～10^5 s^{-1} [22]. The SWID observation object is the solar wind ions in the energy range of 0.04～20 keV. SWID aims to obtain the basic characteristics of the solar wind in lunar space, such as speed, temperature, density, *etc*. The detection results are used to examine the characteristics of the plasma environment in lunar space and the interaction between plasma and the moon.

HPD is composed of three semiconductor silicon detectors, mainly to measure the solar high-energy particle events. The field of view of HPD is 60°, and it can observe 4～400 MeV protons, 0.1～2 MeV electrons, >2 MeV electrons, 13～105 MeV helium, 34～210 MeV lithium, and 117～590 MeV carbon ion[21]. High-energy particles in this range can penetrate the satellite surface, which may cause charging effect, single-event effect,

Table 5 Particle species and energy range of the SEMs of Fengyun geostationary meteorological satellite

	High-energy electrons/MeV	High-energy protons/MeV	Heavy ions
FY-2 A(B)	E : >1.4 MeV	P4: > 1.1 MeV P1: 3.5～26 MeV P2: 10～26 MeV P3: 26～300 MeV	^{3}He, 3.5～26 MeV/n ^{4}He, 3.5～26 MeV/n
FY-2 C(D/E)	E1 : ⩾350 keV E2 : ⩾2.0 MeV	P1: 10～30 MeV P2: 30～100 MeV P3: 100～300 MeV	He, 40～120 MeV Li, 80～240 MeV
FY-2 F(G)	E1: 0.2～0.3 MeV E2: 0.3～0.4 MeV E3: 0.4～0.5 MeV E4: 0.5～0.6 MeV E5: 0.6～0.8 MeV E6: 0.8～1.0 MeV E7: 1.0～1.5 MeV E8⩾1.5 MeV E9⩾2.0 MeV E10⩾3.0 MeV E11⩾4.0 MeV	P1: 4～9 MeV P2: 9～15 MeV P3: 15～22 MeV P4: 22～40 MeV P5: 40～80 MeV P6: 80～165 MeV P7: >165 MeV	He_1, 4～10 MeV/n He_2, 10～20 MeV/n He_3, >20 MeV/n
FY-4 A	E1: 0.4～0.5 MeV E2: 0.5～0.6 MeV E3: 0.6～0.8 MeV E4: 0.8～1.0 MeV E5: 1.0～1.2 MeV E6: 1.2～1.5 MeV E7: 1.5～2.0 MeV E8: 2.0～4.0 MeV E9 >2.0 MeV	P1: 1～2 MeV P2: 2～4 MeV P3: 4～9 MeV P4: 9～15 MeV P5: 15～40 MeV P6: 40～80 MeV P7: 80～165 MeV P8 >165 MeV	

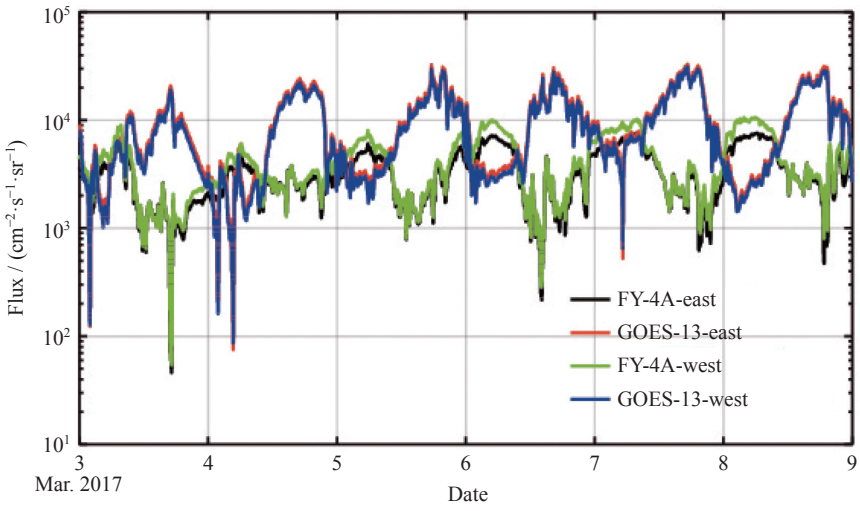


Fig. 9 Fluxes of relativistic electron (> 2 MeV) from FY-4A and GOES-13 from 3 to 9 March 2017

Table 6 Main parameters of particle detectors onboard TC-1/2

	HEED	HEPD	HID
Geometric factor	0.0274 $cm^2 \cdot sr$	0.1105 $cm^2 \cdot sr$	0.255 $cm^2 \cdot sr$
Count rate	0～105 s^{-1}	0～105 s^{-1}	NC
Energy range	0.2～10 MeV	3～400 MeV	12 MeV (He^+)～8 GeV (Fe)
Energy channels	E0: 0.2～0.4 MeV	P1: 3.0～5.0 MeV	He: 12～50 MeV, 50～130 MeV, 130～220 MeV, 220～50 MeV
	E1: 0.4～0.5 MeV	P2: 5.0～10.0 MeV	Li: 23～250 MeV
	E2: 0.5～0.6 MeV	P3: 10～20 MeV	Be: 36～390 MeV
	E3: 0.6～0.8 MeV	P4: 20～30 MeV	B: 53～640 MeV
	E4: 0.8～1.0 MeV	P5: 30～50 MeV	C: 70～700 MeV
	E5: 1.0～1.5 MeV	P6: 50～100 MeV	N: 89～890 MeV
	E6: 1.5～2.0 MeV	P7: 100～200 MeV	O: 109～1090 MeV
	E7: 2.0～3.0 MeV	P8: 200～400 MeV	F: 137～1341 MeV
	E8: 3.0～10.0 MeV		Mg: 200～2000 MeV
			Ar: 380～400 MeV
			Fe: 640～7000 MeV



Fig. 10 Fight model of HEPD onboard TC-1

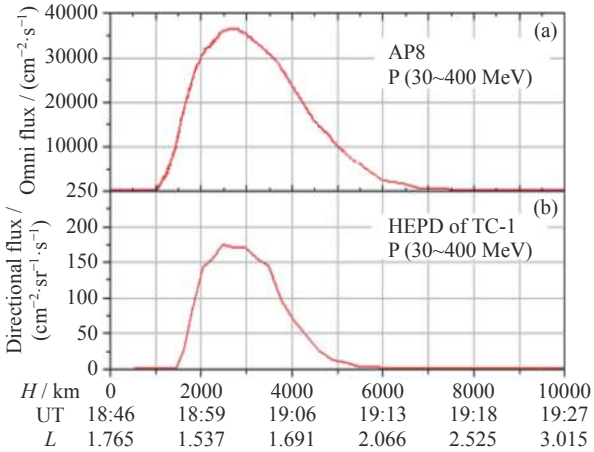


Fig. 11 Comparison between AP8-predicted high-energy proton omni-directional flux and the directional flux of HEPD/TC-1 on January 2004

and so on. These events pose a threat to the normal operation of the satellite. The detection data obtained by SEM is used to study the origin, transmission, and time-space characteristics of high-energy charged particles near the surface of the moon, providing abundant information for the safety of spacecraft design.

A large amount of CE-1 and CE-2 detection data has provided a deep understanding of the near-Lunar space environment. CE-1 and CE-2 monitored many high-energy electron burst events. Wang *et al.*[23] analyzed the typical detection data of HPD and SWID onboard CE-1 and CE-2. The analysis results showed that the energetic particle radiation environment in near-Moon space is not very different from the interplanetary space during the calm period of solar activity and the lunar surface is bombarded by the solar wind. In addition, the sharp increase in the energetic electron flux can cause a significant decrease in the potential of the lunar surface and satellites, leading to particle acceleration events.

The space environment detection of CE-4 is based on an international cooperation method[24]. The lunar Lander Neutron and Dosimetry (LND) instrument on-

board CE-4 is used to measure the integrated particle radiation dose, LET spectrum, fast neutron spectrum, and thermal neutron spectrum on the lunar surface[25]. A picture of LND is shown in Fig.13. The Advanced Small Analyzer for Neutrons (ASAN) instrument is used to measure the energy-neutral atomic flux and distribution function during the scattering process on the lunar surface. The ASAN detection results are used to examine the memory mechanism of the atmospheric sputtering process on the lunar surface[26].

During LND's orbit operation, two solar particle burst events were monitored on 6 May 2019 and 1 December 2020. Zhang *et al.*[27] analyzed the measurement results of the radiation dose of LND on the lunar surface: the average total absorbed dose rate of the lunar surface particle radiation in silicon was 12.66±0.45 μGy·h^{-1}, and the neutral particle absorbed dose rate was 2.67±0.16 μGy·h^{-1}. Fig.14[27] shows the radiation dose

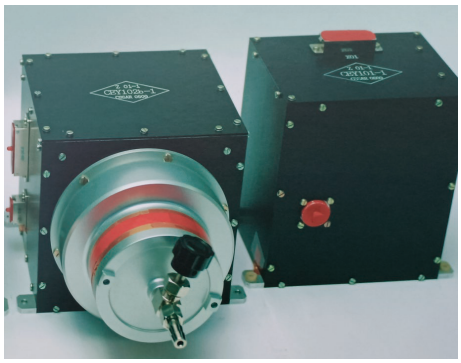


Fig. 12 Solar wind ion detector (left side) and high energy particle detector (right side)

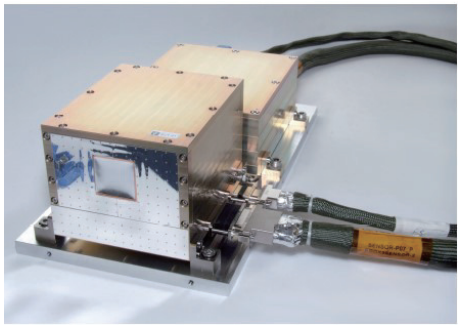


Fig. 13 Lunar lander neutron and dosimetry equipment

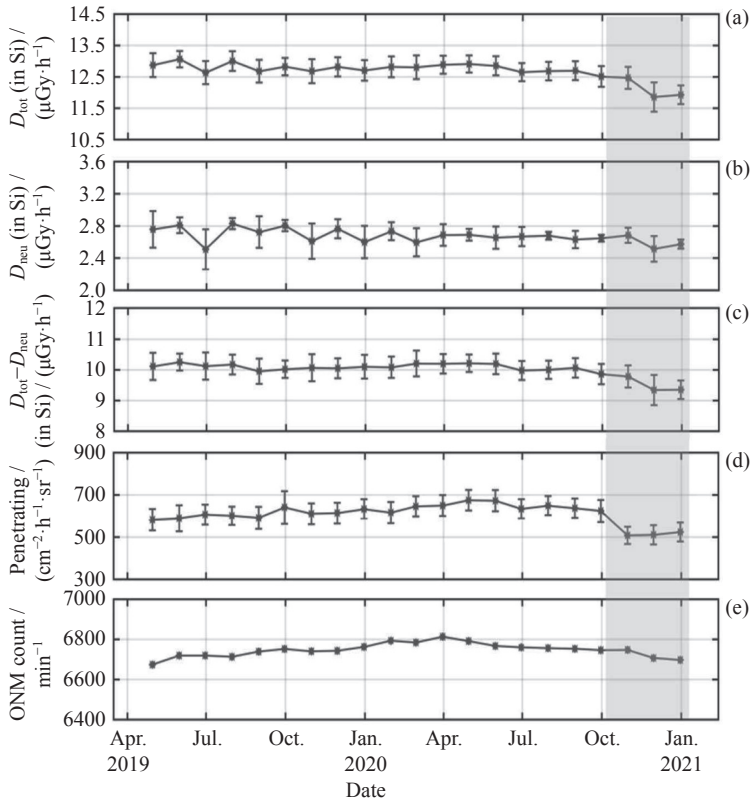


Fig. 14 Temporal evolution of the radiation environment on the Moon as measured by LND on CE-4.
(a) Total radiation dose rate, (b) radiation dose rate of neutral particles, (c) radiation dose rate of charged particles, (d) penetrating flux of high-energy charged particles, and (e) ground measured neutron result

measurement results obtained by LND from May 2019 to January 2021. It can be seen that the total radiation dose rate and the change in the neutral particle radiation dose rate are positively correlated with the flux of the penetrating particles, which conforms to the cognition of space physics.

3 Summary and Outlook

After decades of struggle and development, China is gradually becoming the international leader in space exploration. The CMSP has successfully implemented several missions from Shenzhou-I to Shenzhou-XI, Tiangong-I, Tiangong-II, and the space station Tianhe core module. The first two steps of the Three-Step Strategy of the CMSP have been realized. The third step, *i.e.*, construction of the Chinese space station, has been initiated. The space station Wentian experimental module I and Mengtian experimental module II will also be launched in 2022. The space station orbit construction is being completed gradually. Fengyun series of meteorological satellite data has been used in many fields such as weather forecasting, climate prediction, environmental monitoring, natural disaster warning, and scientific research. It has made outstanding contributions to disaster prevention and reduction, strengthening national economy, national defense construction, and promoting the economic development of many countries. The implementation of DSP has not only improved the Chinese space exploration technology and scientific research level but also enhanced its position in the international space community. China has now completed the missions of rounding, falling, and returning of the CLEP, laying a solid foundation for its future exploration of the moon and planets. Tianwen-1 successfully landed on Mars, facilitating China's leap from the Earth-Moon system to interplanetary space exploration, which is a vital step in interstellar exploration.

Chinese has made outstanding achievements in space environmental exploration. We have gained rich experience for more challenging deep space exploration programs such as lunar, Mars, asteroid, and sun exploration. From the perspective of the universe, the deep-space environment detection path is obstructive and long. Space environment exploration is the basis for improving the ability of aerospace engineers to adapt to the space environment. Improving macro and micro detection capabilities, enhancing long-period multi-target detection capabilities, and improving data transmission capabilities are the development trends of international space environment detection payloads.

References

[1] WANG Tongquan, SHEN Yongping, WANG Shangwu, *et al.* Radiation effects in the space radiation environment[J]. *Journal of National University of Defense Technology*, 1999(4): 36-39 (王同权, 沈永平, 王尚武, 等. 空间辐射环境中的辐射效应[J]. 国防科技大学学报, 1999(4): 36-39)

[2] XU Ying, ZHU Guangwu, WANG Shijin, *et al.* Shenzhou spacecraft space environment monitoring system[J]. *Spacecraft Engineering*, 2004(1): 141-148 (徐颖, 朱光武, 王世金, 等. 神舟飞船空间环境监测系统[J]. 航天器工程, 2004(1): 141-148)

[3] XU Ying, WANG Shijin, ZHU Guangwu, *et al.* Development of space environmental monitors on Chinese manned spacecraft[J]. *Science & Technology Review*, 2010, **28**(8): 110-115 (徐颖, 王世金, 朱光武, 等. 中国载人航天空间环境监测系统的发展[J]. 科技导报, 2010, **28**(8): 110-115)

[4] ZHANG Wei, ZHU Guangwu, WANG Shijin, *et al.* High energy particle detector of Shenzhou spacecraft[C]//Proceedings of the 16 th Academic Conference of the Space Exploration Professional Committee of the Chinese Space Science Society. Beihai: Chinese Society of Space Research, 2003: 20-25 (张微, 朱光武, 王世金, 等. 神舟飞船高能粒子探测器[C]//中国空间科学学会空间探测专业委员会第十六次学术会议论文集(上). 北海: 中国空间科学学会, 2003: 20-25)

[5] YE Zonghai. Space environment studies for the SZ-4 spacecraft[J]. *Physics*, 2004, **33**(1): 40-48 (叶宗海. "神舟"四号中的空间环境研究[J]. 物理, 2004, **33**(1): 40-48)

[6] YANG Xiaochao, WANG Shijin, WANG Yue. Analysis of high energy electron distribution in manned space orbit[C]//Proceedings of the 16th Academic Conference of the Space Exploration Professional Committee of the Chinese Space Science Society. Beihai: Chinese Society of Space Research, 2003: 189-193 (杨晓超, 王世金, 王月. 载人航天轨道高能电子分布情况分析[C]//中国空间科学学会空间探测专业委员会第十六次学术会议论文集(上). 北海: 中国空间科学学会, 2003: 189-193)

[7] SHEN Guohong, WANG Shijin, ZHANG Shenyi, *et al.* A particles' direction detector on manned space II[J]. *Nuclear Electronics & Detection Technology*, 2012, **32**(5): 535-538 (沈国红, 王世金, 张申毅, 等. 二期载人航天空间粒子方向探测器[J]. 核电子学与探测技术, 2012, **32**(5): 535-538)

[8] CMS. About CMS[EB/OL]. [2021-06-06]. http://en.cmse.gov.cn/aboutcms/

[9] YANG J, ZHANG Z Q, WEI C Y, *et al*. Introducing the new generation of Chinese geostationary weather satellites, Fengyun-4[J]. *Bulletin of the American Meteorological Society*, 2017, **98**(8): 1637-1658

[10] WANG Shijin, ZHU Guangwu, LIANG Jinbao, *et al*. FY-1 C space particle composition monitor and its detection results[C]//Proceedings of the Twelfth Academic Conference of the Space Exploration Professional Committee of the Chinese Society of Space Sciences. Kunming: Space Exploration Professional Committee of Chinese Society for Space Science, 1999: 121-124 (王世金, 朱光武, 梁金宝, 等. FY-1 C空间粒子成分监测器及其探测结果[C]//中国空间科学学会空间探测专业委员会第十二次学术会议论文集. 昆明: 中国空间科学学会空间探测专业委员会, 1999: 121-124)

[11] DONG C H, YANG J, ZHANG W J, *et al*. An overview of a new Chinese weather satellite FY-3 A[J]. *Bulletin of the American Meteorological Society*, 2009, **90**(10): 1531-1544

[12] LI Jiawei, HUANG Cong, YU Chao, *et al*. Inspection and application of energetic particles data of FY-3 C/SEM satellite[J]. *National Remote Sensing Bulletin*, 2018, **22**(1): 76-86 (李嘉巍, 黄聪, 于超, 等. 风云三号C星SEM高能粒子数据检验及应用[J]. 遥感学报, 2018, **22**(1): 76-86)

[13] RIPOLL J F, CLAUDEPIERRE S G, UKHORSKIY A Y, *et al*. Particle dynamics in the Earth's radiation belts: review of current research and open questions[J]. *Journal of Geophysical Research: Space Physics*, 2020, **125**(5): e2019JA026735

[14] WANG Chunqin, ZHANG Xin, ZHANG Liguo, *et al*. Space radiation environment observations and applications based on GEO satellites[J]. *Aerospace Shanghai*, 2017, **34**(4): 85-95 (王春琴, 张鑫, 张立国, 等. 地球同步轨道系列卫星自主空间辐射环境监测及应用[J]. 上海航天, 2017, **34**(4): 85-95)

[15] LIU Zhen, YANG Xiaochao, ZHANG Xiaoxin, *et al*. On-orbit cross-calibration and assimilation for relativistic electron observations from Fengyun-4A and GOES-13[J]. *Acta Physica Sinica*, 2019, **68**(15): 159401 (刘震, 杨晓超, 张效信, 等. 风云四号A星和GOES-13相对论电子观测数据在轨交叉定标及数据融合研究[J]. 物理学报, 2019, **68**(15): 159401)

[16] LIU Z X, ESCOUBET C P, PU Z, *et al*. The Double Star mission[J]. *Annales Geophysicae*, 2005, **23**(8): 2707-2712

[17] DUNLOP M W, ESCOUBET C P, LIU Z X, *et al*. Double star: mission, instruments and joint observations[M]//LAAKSO H, TAYLOR M, ESCOUBET C P. The Cluster Active Archive. Dordrecht: Springer, 2010: 331-346

[18] CAO J B, LIU Z X, YAN C X, *et al*. First results of Chinese particle instruments in the Double Star program[J]. *Annales Geophysicae*, 2005, **23**(8): 2775-2784

[19] LIU Zhenxing. Geospace Double Star exploration project[J]. *Chinese Journal of Geophysics*, 2001, **44**(4): 573-580 (刘振兴. 地球空间双星探测计划[J]. 地球物理学报, 2001, **44**(4): 573-580)

[20] OUYANG Z Y, LI C L, ZOU Y L, *et al*. Chang'E-1 lunar mission: an overview and primary science results[J]. *Chinese Journal of Space Science*, 2010, **30**(5): 392-403,391

[21] WANG Xinyue, JING Tao, ZHANG Shenyi, *et al*. The first results of Chang'E-1 high energetic particles detector[J]. *Progress in Geophysics*, 2012, **27**(6): 2289-2295 (王馨悦, 荆涛, 张珅毅, 等. "嫦娥一号"卫星太阳高能粒子探测器的首次观测结果[J]. 地球物理学进展, 2012, **27**(6): 2289-2295)

[22] WANG Chi, ZHANG Xianguo, XU Xinfeng, *et al*. The lunar and deep space environment exploration in China[J]. *Journal of Deep Space Exploration*, 2019, **6**(2): 105-118 (王赤, 张贤国, 徐欣锋, 等. 中国月球及深空空间环境探测[J]. 深空探测学报, 2019, **6**(2): 105-118)

[23] WANG Xinyue, ZHANG Aibing, JING Tao, *et al*. The lunar charged particle environment by Chang'E-1 and Chang'E-2[J]. *Journal of Deep Space Exploration*, 2019, **6**(2): 119-126 (王馨悦, 张爱兵, 荆涛, 等. 近月空间带电粒子环境——"嫦娥1号""嫦娥2号"观测结果[J]. 深空探测学报, 2019, **6**(2): 119-126)

[24] LI C L, ZUO W, WEN W B, *et al*. Overview of the Chang'E-4 mission: opening the frontier of scientific exploration of the lunar far side[J]. *Space Science Reviews*, 2021, **217**(2): 35

[25] JIA Y Z, ZOU Y L, PING J S, *et al*. The scientific objectives and payloads of Chang'E-4 mission[J]. *Planetary and Space Science*, 2018, **162**: 207-215

[26] YE Peijian, SUN Zezhou, ZHANG He, *et al*. Mission design of Chang'E-4 probe system[J]. *Scientia Sinica:Technologica*, 2019, **49**(2): 124-137 (叶培建, 孙泽洲, 张熇, 等. 嫦娥四号探测器系统任务设计[J]. 中国科学:技术科学, 2019, **49**(2): 124-137)

[27] ZHANG Shenyi, HOU Donghui, WIMMER-SCHWEINGRUBER R F, *et al*. Radiation dose of LND on the lunar surface in two years[J]. *Chinese Journal of Space Science*, 2021, **41**(3): 439-444 (张珅毅, 侯东辉, WIMMER-SCHWEINGRUBER R F, 等. LND两年月表辐射剂量测量结果[J]. 空间科学学报, 2021, **41**(3): 439-444)